



## Research article

Using ethanol for continuous biodiesel production with trace catalyst and CO<sub>2</sub> co-solvent

Aso A. Hassan, Hayder A. Alhameedi, Joseph D. Smith\*

Chemical and Biochemical Engineering, Missouri University of Science &amp; Technology, USA



## ARTICLE INFO

Keywords  
Biodiesel  
Supercritical ethanol  
Kinetic model  
CO<sub>2</sub> co-solvent

## ABSTRACT

The continuous biodiesel production process under sub- and supercritical conditions using a trace amount of potassium hydroxide (KOH) as a catalyst has been studied. CO<sub>2</sub> was added as a co-solvent to reduce the reaction time and increase biodiesel yield. The proposed procedure enables simultaneous transesterification and esterification of triglycerides and free fatty acid (FFA), respectively. The shorter reaction time and milder reaction conditions may reduce energy consumption due to the simplification of the separation and purification steps. The process variables, including reaction temperature, ethanol to oil molar ratio, catalyst amount, and process pressure, were systematically optimized. The highest biodiesel yield (98.12%) was obtained after a 25-min reaction time using only 0.11% wt. of KOH and a 20:1 ethanol to oil ratio. The process optimum temperature and pressure were 240 °C and 120 bar, respectively. The proposed kinetic model suggested a first-order reaction with an activation energy of 15.7 kJ mol<sup>-1</sup> and a reaction rate constant of 0.0398/min<sup>-1</sup>. The thermodynamic parameters such as Gibbs free energy, enthalpy, and entropy were calculated as 144.82 kJ mol<sup>-1</sup>, 11.4 kJ mol<sup>-1</sup>, and -0.26 kJ mol<sup>-1</sup> at 240 °C, respectively.

## 1. Introduction

Biodiesel is a mono-alkyl ester compound derived from the reaction of renewable sources such as vegetable oil or animal fat with short-chain alcohols like methanol and ethanol. Recently, other bioresources have also been used for biodiesel production, such as waste cooking oil [1–6], sludge waste [7,8], and algal oil [9–12]. Biodiesel is biodegradable, non-toxic, and has a lower emission profile than petroleum diesel. Therefore, biodiesel is accounted as an environmentally friendly product. For instance, biodiesel can reduce 78% of the CO<sub>2</sub> and 90% of the smoke emissions and eliminate sulfur dioxide emission. Furthermore, biodiesel has a higher energy content among other fuels such as gasoline, methanol, and ethanol. For example, 1 gal of pure biodiesel (B100) has 103% of the energy of 1 gal of gasoline, while 1 gal of ethanol has 73% of 1 gal of gasoline energy (see Table 1) [13,14].

The most common method for biodiesel production is through transesterification reactions of oils with alcohol (see Figs. 1 and 2) under a homogeneous or heterogeneous catalyst of alkali [15,16], acid [17,18] or enzyme [19,20]. The alkali catalyst has a high reaction rate at low temperature and pressure. However, with poor quality feedstocks that contain high percentages of free fatty acid (FFA) and water, the alkali catalyst will react with the FFA to form soaps, which make the downstream steps in biodiesel production process very sophisticated

(see Fig. 3). On the other hand, the homogeneous/heterogeneous acid and enzyme catalysts could be used for poor-quality feedstocks with high FFA and water contents, but the reaction rate is much slower, and the product yield is slightly lower [21,22]. Furthermore, the conventional catalyzed process has been criticized because the catalyst washing out step produces a large amount of wastewater that must be treated before being reused [23].

According to the most recent literature, the non-catalytic processes (see Fig. 1) decrease the process mass-transfer limitation, improve the reaction phase solubility, and make the product separation and purification steps easier. It has been shown that the non-catalytic supercritical process affords higher reaction rates and is tolerant to poor-quality feedstocks [24–27].

However, the supercritical method requires high temperature, pressure, and alcohol/oil ratios for the reaction to present high yield levels, which leads to high processing costs and, in some cases, causes product thermal decomposition that reduces the reaction conversion. In order to achieve high reaction conversions at milder temperatures and pressures, and shorter reaction times to prevent thermal decomposition of the products, attempts have been made through the addition of co-solvent [28,29] and trace amounts of the catalyst [21,30,31] to improve the reaction conditions. The response surface methodology (RSM) and/or artificial neural network (ANN) based approaches can be used

\* Corresponding author.  
E-mail address: [smithjose@cmst.edu](mailto:smithjose@cmst.edu) (J.D. Smith).

<https://doi.org/10.1016/j.fuproc.2020.106377>

Received 30 September 2019; Received in revised form 4 February 2020; Accepted 11 February 2020

Available online 09 March 2020

0378-3820/© 2020 Elsevier B.V. All rights reserved.

**Table 1**  
Fuel properties comparison.

	Gasoline/E10	Low sulfur diesel	Biodiesel (B100)	Ethanol (E100)	Methanol	Natural gas	Hydrogen
Chemical structure	C <sub>2</sub> to C <sub>12</sub> and ethanol ≤ 10% 112–116 Btu/gal	C <sub>8</sub> to C <sub>25</sub>	Methyl ester of C <sub>12</sub> to C <sub>22</sub> fatty acids	CH <sub>3</sub> CH <sub>2</sub> OH	CH <sub>3</sub> OH	CH <sub>4</sub> with inert gas < 0.5%	H <sub>2</sub>
Energy content (lower heating value)	120–124 Btu/gal	129 Btu/gal	120 Btu/gal	76 Btu/gal	57 Btu/gal	21 Btu/lb.	52 Btu/lb.
Energy content (higher heating value)	120–124 Btu/gal	139 Btu/gal	128 Btu/gal	85 Btu/gal	65 Btu/gal	24 Btu/lb.	61 Btu/lb.
Physical state	Liquid	Liquid	Liquid	Liquid	Liquid	Cryogenic liquid	Compressed gas or liquid
Cetane number	N/A	40–55	48–65	0–54	N/A	N/A	N/A
Octane number	84–93	N/A	N/A	110	112	120	130
Flash point (°F)	–45	165	212–338	55	52	–306	N/A
Autoignition temperature (°F)	495	600	300	793	897	1004	1050–1080
Gasoline gallon equivalent	97%–100%	1 gal has 113% energy of 1 gal of gasoline	1 gal has 103% energy of 1 gal of gasoline	1 gal has 73% energy of 1 gal of gasoline	1 gal has 49% energy of 1 gal of gasoline	5.38 lbs. have 100% energy of 1 gal of gasoline	2.198 lbs. have 100% energy of 1 gal of gasoline
Energy, security impacts	Manufacture using oil, of which nearly 1/2 is imported	Manufacture using oil, of which nearly 1/2 is imported	Domestically produce from renewable sources and reduces 95% of petroleum use throughout its lifecycle	Domestically produce from renewable sources and reduces 70% of petroleum use throughout its lifecycle	Domestically produce from natural gas, coal, or woody biomass	Produce from underground reserves and renewable biogas	Produce from natural gas, methanol, and water electrolysis

successfully for process modeling, optimization, and intensification to establish sustainable and less-energy-intensive methods. To the best of the author's knowledge, the kinetics and optimization of the SCE transesterification process with co-solvent and trace amounts of catalyst have not been studied previously. The proposed method combines the advantages of supercritical techniques with the base-catalyzed method, which means it needs lower reaction conditions such as lower alcohol/oil molar ratio, lower catalyst amounts with minimal undesired reactions, and much shorter reaction times. Process variables, including temperature, pressure, alcohol/oil molar ratio, and catalyst amount, were optimized. The process kinetics and thermodynamic study were also discussed.

## 2. Experimental section

The experimental setup system from the previous reports was modified for carbon dioxide and trace catalyst amount addition.

### 2.1. Materials

The WCO was collected from different sources and mixed before the transesterification process. The properties of the collected oil are compared to virgin vegetable oil in Table 2, and the oil chemical composition is reported in Table 3. The WCO samples were filtered to remove all undesirable and insoluble impurities, such as suspended particulate materials. Then, the samples were heated to 50 °C for 10 min to lower the moisture content (i.e., water). Sigma-Aldrich supplied other solvents and reagents, such as 99.9% pure analytical grade ethanol and pure grade catalyst pellets (KOH) that were used without any further purification. Carbon dioxide (99.9%) was used as a co-solvent without further treatment.

The first number in the carbon atom structure in column 2 of Table 3 is the carbon atom number, and the second number is the double bond number.

### 2.2. Process setup and experimental procedure

The reactor was constructed from 316 SS tubing. The reactor dimensions are 264 in. length, 1/8 in. the outside diameter and 0.040 in. the inside diameter. The two-reactor ends are coned, and threaded nipples are provided with high-pressure connections (as shown in Fig. 4).

The process setup is illustrated in Fig. 5. Section 1 is the mixing section that contains a 1000 ml Pyrex container, an electrical stir heater plate, a heat exchanger (condenser), and a chiller for cooling the recycled alcohol, and temperature controller. Section 2 is the high-pressure pumping section that includes the reciprocating high-pressure pump (Teledyne 6010R), two-way valve, one-way soft seat check valve, pressure, and flow controllers. Section 3 is the reactor section that contains the reactor (as shown in Fig. 4), two-way valve, one-way soft seat check valve, two semi-cylinder electrical heaters, CO<sub>2</sub> cylinder, temperature controller, and two temperature transmitters. Finally, Section 4 is the collecting section that includes the product and by-product condenser and chiller, a collection container, temperature transmitter, and backpressure regulator. Fig. 5 also shows each stream diameter, the materials that they are made from, and the service materials. For example, 0.5-H<sub>2</sub>O-Tef-N means 0.5 in. outside diameter, service water, made from Teflon material, and normal pressure, respectively.

The ethanol, oil, and a specified amount of the catalyst were mixed in the Pyrex container (Section 1) for 20 min at 60 °C, which is lower than the ethanol boiling point (78.37 °C). Then, the sample was pumped to the reactor by the high-pressure liquid chromatographic pump. The total flow rate range was 1–10 ml/min, depending on the residence time and the ethanol/oil molar ratio. The co-solvent (CO<sub>2</sub>) was added to the system at 40 bar. After the reaction took place, the product and the

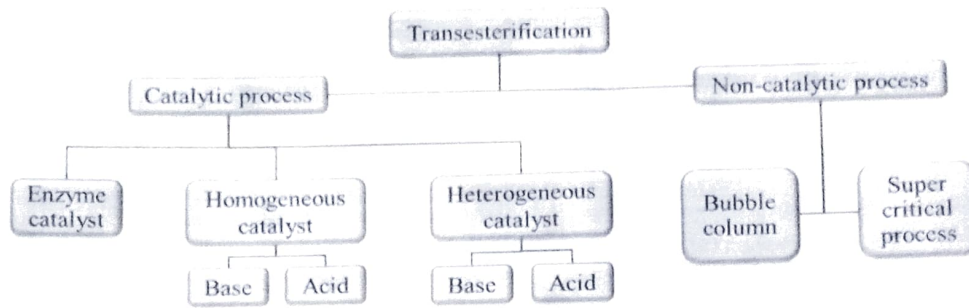


Fig. 1. The transesterification processes.

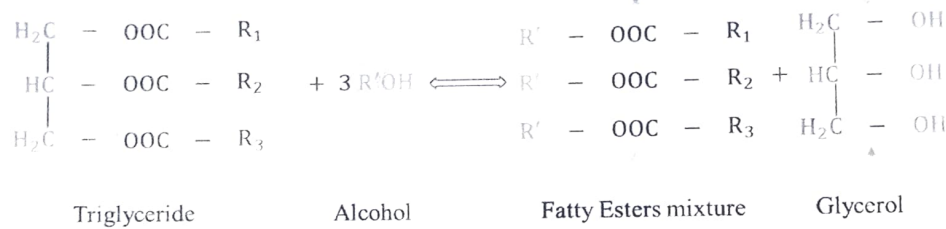


Fig. 2. The transesterification reaction mechanism.

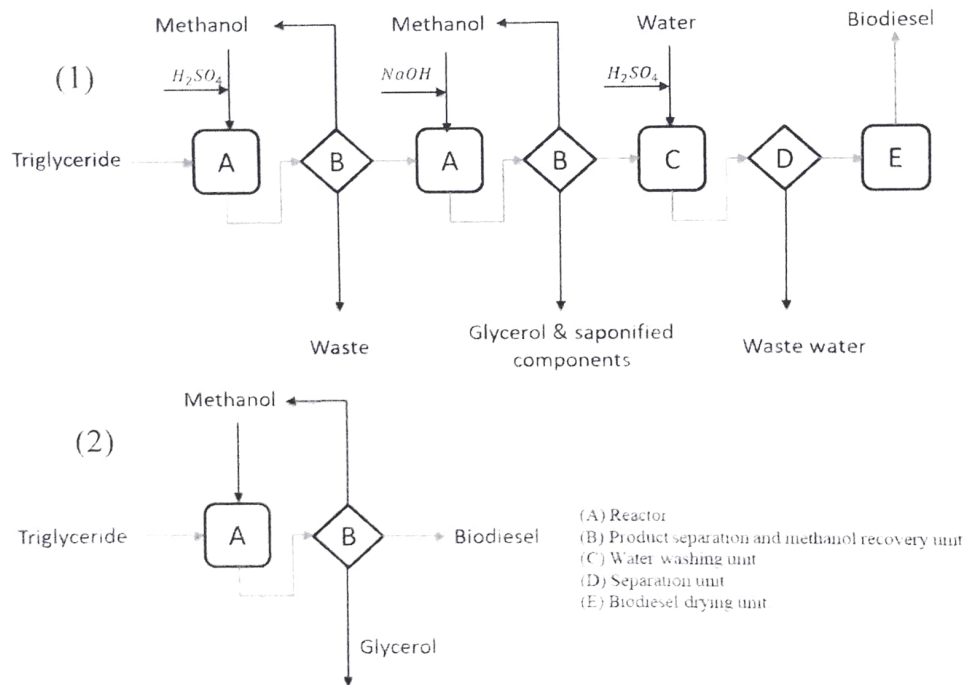


Fig. 3. The catalyzed process (1) & the super-critical methanol process (2).

Table 2  
The WCO and virgin oil properties.

Property	WCO	Virgin vegetable oil
Saponification value (SV)	197.8	195.4
FFA contents (%)	23.26	0.87
Kinematic viscosity (mm <sup>2</sup> /s)	38.6	32.5
Density @ 15 °C (kg/m <sup>3</sup> )	944	914
Flashpoint (°C)	239	209
Acid value (mg KOH/g)	2.3	0.4

Table 3  
The fatty acid weight concentration of virgin oil and collected WCO.

Fatty acid	Structure	WCO (wt%)	Virgin oil (wt%)
Palmitic acid	C16:0	3.8	9.2
Palmitoleic acid	C16:1	3.1	0.68
Stearic acid	C18:0	2.7	4.2
Oleic acid	C18:1	43.7	30.6
Linoleic acid	C18:2 (cis)	34.7	51.1
Linolenic acid	C18:3	9.5	4.2

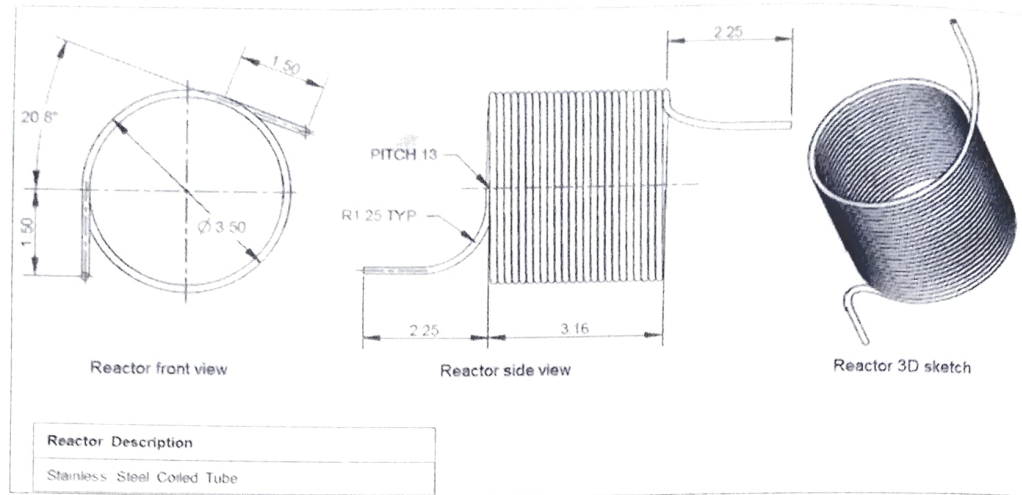


Fig. 4. Reactor dimension.

by-product were cooled in the condenser and depressurized using a backpressure regulator. Approximately 20 ml of the liquid product samples were collected.

2.3. Alcohol recovery and samples analysis

The liquid product sample was treated in the alcohol recovery system to recover excess ethanol. Then, the sample was left overnight to achieve complete separation between the glycerol (lower layer) and the biodiesel (upper layer).

Standard gas-chromatography (GC) methods determine if the biodiesel conforms to the standard specifications, one of which determines the ethyl ester content (EN-14103). The ethyl ester concentration was analyzed using an Agilent 7890A gas chromatography equipped with an HP-INNOWAX column (30 m × 0.25 ml). Approximately 250 mg of a product sample is weighted in 10 ml of the vial, then 5 ml of methyl heptadecanoate solution (5 mg/ml solution of methyl heptadecanoate in heptane) was added to the sample using a pipette. The oven temperature was held for 9 min at 210 °C as an isothermal period, and then the oven was heated at 20 °C/min to 230 °C and held for 10 min. The ester content ( $C_{ester}$ ), expressed as a mass fraction in percent, was calculated using Eq. (1). The methyl ester yield in each experiment was calculated by Eq. (2).

$$C_{ester} = \frac{\sum A - PM}{PM} \times \frac{MC \times MV}{m} \times 100 \tag{1}$$

where

- ΣA = the sum of the FAME peak area from C14:0 to C24:1
- PM = peak area of methyl heptadecanoate.
- MC = methyl heptadecanoate solution concentration (mg/ml)
- MV = methyl heptadecanoate solution volume (ml)
- m = mass of the sample (mg)

$$yield\% = C_{ester} \times \frac{V_{product}}{V_{oil\ fed}} \times 100 \tag{2}$$

where

- $V_{product}$  = biodiesel volume
- $V_{oil - fed}$  = oil volume
- $C_{ester}$  = ester content from Eq. (1)

2.4. Experimental design

The response surface methodology that combines mathematical and statistical methods is the typical method for optimizing many chemical processes and is useful for modeling and analyzing interest response, which is affected by several variables [32]. The selected independent variables for the present work were the following:

1. Temperature ( $x_1$ )
2. Reaction time ( $x_2$ )
3. The ethanol-to-oil molar ratio ( $x_3$ )
4. Catalyst amount (wt%) ( $x_4$ )
5. Pressure ( $x_5$ )

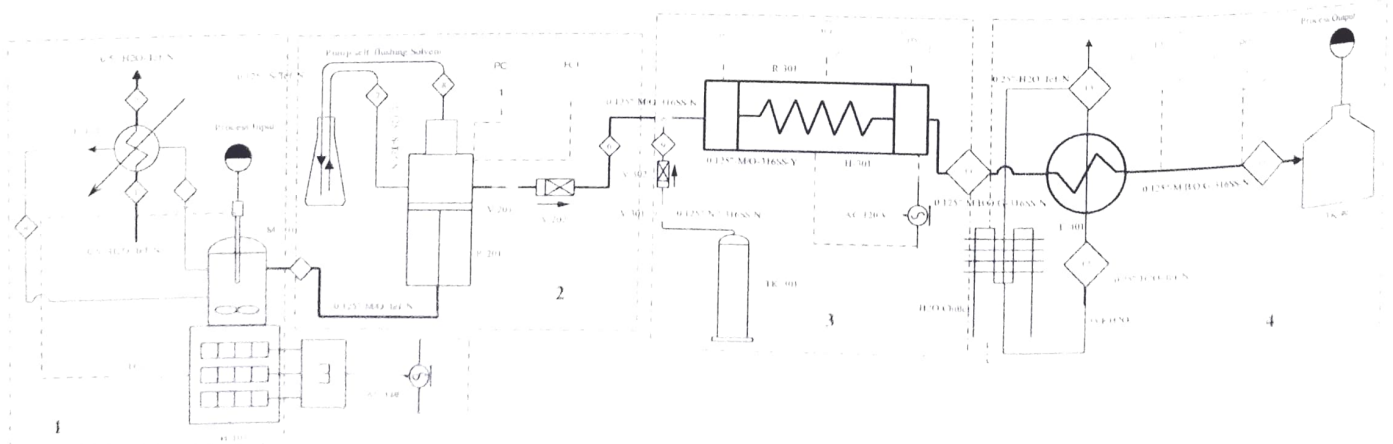


Fig. 5. Schematic diagram of the experimental setup.

**Table 4**  
The matrix of five independent variables.

Un-coded variables					Coded variables				
Temperature (°C)	Time (min)	Molar ratio	Catalyst (wt%)	Pressure (bar)	$x_1$	$x_2$	$x_3$	$x_4$	$x_5$
200	10	10	0.01	40	-1	-1	1	1	1
200	40	10	0.01	40	-1	1	1	1	0
280	40	10	0.01	80	1	1	1	1	1
280	40	30	0.01	120	1	1	1	1	1
280	10	10	0.11	40	1	1	1	1	1
280	40	10	0.11	40	1	1	1	1	1
280	10	30	0.11	120	1	1	1	1	1
280	10	10	0.01	40	1	-1	1	1	1
200	10	30	0.01	40	1	-1	1	1	1
280	10	30	0.01	120	1	-1	1	1	1
200	40	30	0.01	40	1	1	1	1	1
200	10	10	0.11	40	1	1	1	1	1
200	40	10	0.11	40	1	1	1	1	1
200	10	30	0.11	40	1	1	1	1	1
200	40	30	0.11	40	1	1	1	1	1
240	25	20	0.06	80	0	0	0	0	0
240	25	20	0.06	80	0	0	0	0	0
240	25	20	0.06	80	0	0	0	0	1
240	25	20	0.06	120	0	0	1	0	1
240	25	10	0.06	120	0	0	1	1	1
240	25	10	0.11	120	0	0	1	1	1
240	25	20	0.11	120	0	0	0	1	0
240	25	20	0.11	80	0	0	0	1	0
240	40	20	0.01	80	0	1	0	1	0
240	40	30	0.01	80	0	1	1	1	0
240	25	20	0.01	80	0	0	0	1	0
240	25	20	0.01	120	0	0	0	1	1
200	10	10	0.01	40	1	-1	1	1	1

The fatty acid ethyl ester (FAEE) yield was the dependent variable (y). In the present study, the independent parameters and their levels were selected based on preliminary experiments carried out in the laboratory. The quadratic regression model was used to explore the effect of the independent variables on the response [32].

$$y = \beta_0 + \sum_{i=1}^4 \beta_i x_i + \sum_{i=1}^4 \beta_{ii} x_i^2 + \sum_{i=1}^3 \sum_{j=i+1}^4 \beta_{ij} x_i x_j \quad (3)$$

where y is the predicted value of the FAEE yield, and  $\beta_0$ ,  $\beta_i$ ,  $\beta_{ii}$ , and  $\beta_{ij}$  are intercept constant, linear, quadratic, and interactive coefficients between variables i and j, respectively. The method of least squares with Excel, JMP, and MATLAB software was used for regression analysis of the experimental data and 3D plotting of the variables. The model's fitting was verified by the correlation coefficient (R<sup>2</sup>) and the adjusted R<sup>2</sup> coefficient determination. Ideally, the R<sup>2</sup> value is a unity that represents the complete agreement between the predicted and the experimental responses [33,34]. The experiments were carried out to find the optimum values and study the effect of process variables on the FAEE yield, and the results are shown in Table 4. Three-dimensional and contour plots were made by changing any two variables and keeping the other variables constant.

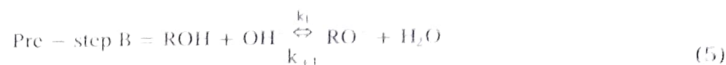
### 3. Kinetic model for waste cooking oil (WCO) transesterifications

#### 3.1. Based-catalyzed transesterifications

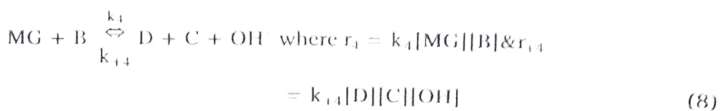
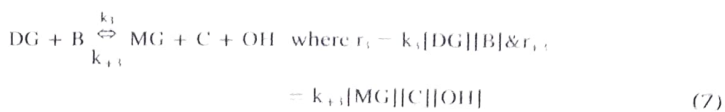
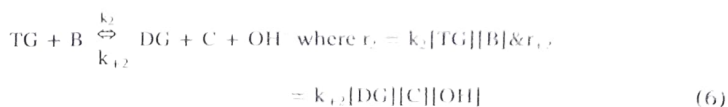
The simple stoichiometric equation for transesterification reaction is



A is waste cooking oil, B is alcohol, and a base catalyst solution (i.e., ROH + OH<sup>-</sup>), C is glycerol, and D is a fatty acid ester (i.e., biodiesel = RCOOR). Moreover, the catalyst and alcohol solution produces an ionic solution according to the alkoxide reaction:

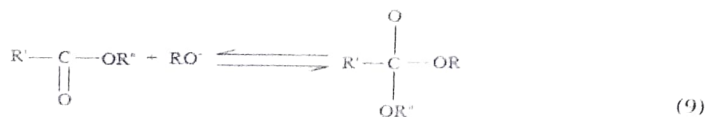


Eq. (5) is a reversible reaction, which can proceed in either direction with  $k_1$  representing the forward reaction rate constant and  $k_{-1}$  is the reverse reaction rate constant. The transesterification reaction scheme approximated as



Eqs. (9), (10), and (11) describe the base-catalyzed transesterification mechanism of the triglyceride molecule by alkoxide ions (RO<sup>-</sup>). In the first step, the RO<sup>-</sup> ion attacks the carbonyl carbon of the triglyceride molecule to produce a tetrahedral intermediate that reacts with the alcohol to generate the RO<sup>-</sup> ion in the second step. In the final step, the tetrahedral intermediate rearrangement gives rise to ester and diglyceride [35].

1st step:



2nd step:



R' = fatty acid carbon chain  
R = alcohol alkyl group

With the exception of the alcoholysis reaction, the undesirable saponification reaction of FFA produces soap (S) and water (W)



Free KOH cannot esterify sodium or potassium based salt or soap (S). Therefore, Eq. (12) is considered to be irreversible. The RO<sup>-</sup> ions represent the active ingredient in the alcoholysis reactions (i.e., Eqs. (6), (7), and (8)), while the OH<sup>-</sup> ions represent the active ingredient in the competing saponification reaction (i.e., Eq. (12)). Thus, the saponification reaction not only consumes the reactants that reduce biodiesel production but also consumes the catalyst needed for the desired reaction. In summary, the base catalyzed transesterification mechanism includes the formation of alkoxide ions (RO<sup>-</sup>) in the pre-step (i.e., Eq. (5)), and then attacks the carbonyl carbon of the TG molecule, producing a tetrahedral intermediate (i.e., Eq. (9)). The reaction between an alcohol and this intermediate product results in the growth of the alkoxide ion, subsequently giving rise to the amount of fatty acid ester [36].

### 3.2. Acid catalyzed esterification

At the supercritical point, alcohol acts as an acid catalyst that esterifies the FFA in the waste cooking oil. This process includes the FFA (i.e., carboxylic acid) esterification, which is a relatively fast reaction, followed by transesterification of TG [6]. Usually, WCO contains a high FFA percentage that is esterified first by alcohol to produce ester, as shown below in Figs. 6 and 7 [37].

#### 3.2.1. Kinetics model

Transesterification reactions use 3 mol of B with 1 mol of A to form

3 mol of C and 1 mol of D. This reaction model consists of three reversible reactions where the monoglycerides (MG) and diglycerides (DG) are intermediate products with 3 mol of FAF being produced as shown and explained in Eqs. (4)–(8) [38].

#### 3.2.1. Initial assumption

In this work, the following assumptions were made:

1. The FFA saponification reaction (Eq. (12)) was not significant since, at the supercritical point, the esterification reaction is a very fast reaction, and the catalyst amount is very small. Therefore, alcoholysis is the only possibly occurring reaction.
2. The assumption that the initial reaction mixture containing only TG is no longer valid since the frying process occurs at high temperatures. These temperatures cause many reactions, such as TG hydrolysis, which leads to higher DG and MG [39].

The kinetic equations for each component are as follows:

$$\frac{d[\text{TC}]}{dt} = r_1 + r_2 \quad (13)$$

$$\frac{d[\text{DG}]}{dt} = -r_1 + r_3 - r_2 + r_5 \quad (14)$$

$$\frac{d[\text{MG}]}{dt} = r_1 - r_3 - r_4 + r_5 \quad (15)$$

$$\frac{d[\text{D}]}{dt} = r_4 - r_5 \quad (16)$$

$$\frac{d[\text{C}]}{dt} = r_1 + r_2 - r_3 + r_4 - r_5 \quad (17)$$

$$\frac{d[\text{B}]}{dt} = -r_1 + r_3 - r_4 + r_5 \quad (18)$$

If Eqs. (13), (14), (15), and (16) are summed up, the opposite sign coefficient, cancel out, and the first balanced equation will be

$$\frac{d[\text{TC}]}{dt} + \frac{d[\text{DG}]}{dt} + \frac{d[\text{MG}]}{dt} + \frac{d[\text{D}]}{dt} = 0 \Leftrightarrow \frac{d[\text{TC} + \text{DG} + \text{MG} + \text{D}]}{dt} = 0 \quad (19)$$

$$[\text{TC} + \text{DG} + \text{MG} + \text{D}] = \text{constant (C')} \quad (20)$$

Moreover, Eqs. (17) and (18) show that the rate of biodiesel product accumulation is equal in magnitude to the rate of alcohol depletion, and can be shown by

$$\frac{d[\text{C}]}{dt} + \frac{d[\text{B}]}{dt} = 0 \Leftrightarrow \frac{d[\text{C} + \text{B}]}{dt} = 0 \quad (21)$$

$$[\text{C} + \text{B}] = \text{C}'' \quad (22)$$

First of all, the integration constant (i.e., C') must be equal to one of the initial concentration of TC, DG, and MG because the total fatty acid

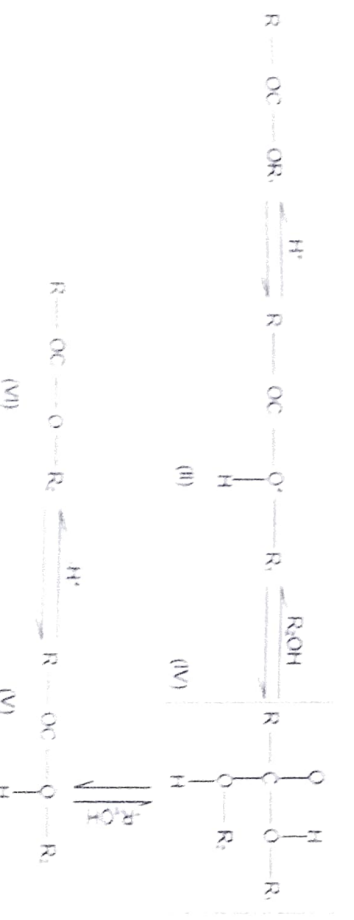


Fig. 6. Mechanism of TG transesterification.

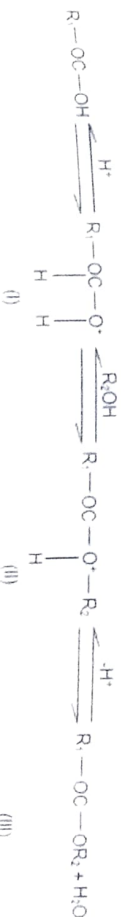


Fig. 7. The FFA esterification.

Table 5  
Experimental design matrix.

Observation	Coded variables			FAEE yield (%)			
	Temperature	Time	Molar ratio	Catalyst	Pressure	Experimental	Predicted
1	-1	-1	-1	-1	-1	35.99	38.298
2	-1	1	-1	-1	-1	44.47	46.346
3	1	1	-1	-1	0	87.3	86.268
4	1	1	1	-1	1	91.45	91.318
5	1	-1	-1	1	-1	84.3	82.585
6	1	1	-1	1	-1	90.65	90.633
7	1	-1	1	1	-1	96.43	97.004
8	1	1	1	1	-1	67.12	68.852
9	-1	-1	-1	-1	-1	32.65	30.418
10	1	1	1	-1	1	82.68	83.27
11	-1	-1	1	-1	-1	53.21	52.031
12	-1	-1	-1	1	-1	62.23	60.079
13	-1	1	-1	1	-1	44.23	44.152
14	-1	1	1	1	-1	54.23	52.2
15	-1	-1	1	1	-1	71.45	72.911
16	0	0	0	0	0	72.56	72.911
17	0	0	0	0	0	73.23	72.911
18	0	0	0	0	0	86.23	85.841
19	0	0	0	0	1	89.89	88.784
20	0	0	0	0	1	94.23	96.461
21	0	0	-1	1	1	98.12	99.404
22	0	0	0	0	0	80.45	83.531
23	0	0	0	0	0	78.56	78.738
24	0	1	1	1	0	73.98	73.802
25	0	0	0	-1	0	73.34	69.797
26	0	0	0	-1	1	85.78	82.727
27	0	0	0	-1	1		

composition weight percent in WCO is equal to 100%. Second, the sum of the ester molecules and the alcohol molecules must equal the initial alcohol molecule quantity (i.e.,  $[B]_0$ ), since alcohol molecules are only consumed to make alkyl esters [40]. Accordingly, rearrangement of Eqs. (20) and (22) gives

$$[TG + DG + MG]_0 = [A]_0 = CA_0 \quad (23)$$

$$[C + B] = [B]_0 = CB_0 \quad (24)$$

In addition, the glyceride concentration (i.e.,  $[TG + DG + MG]_0 = [A]$ ) at any moment of the reaction can be determined by  $C_A = C_{A0}(1 - x)$ , and the fatty acid ester concentration at any moment can be determined by  $C = xC_{A0}$ . Therefore, Eqs. (23) and (24) will be rearranged as

$$[TG + DG + MG] = [A] = C_A = C_{A0}(1 - x) \quad (25)$$

$$[B] = C_B = CB_0 - xC_{A0} \quad (26)$$

The alcohol concentration was assumed to be constant since the reaction contained an excess amount of the alcohol, so Eq. (24) will be  $[B] = C_B = CB_0$

The reaction rate equation can be written as follows:

$$-r_A = k_a C_A^n C_B^m = k C_A^n \quad (28)$$

$$-r_A = -\frac{dC_A}{dt} = -\frac{d[C_{A0}(1-x)]}{dt} = C_{A0} \frac{dx}{dt} = k [C_{A0}(1-x)]^n \quad (29)$$

$$\frac{dx}{dt} = \frac{k}{C_{A0}} [C_{A0}(1-x)]^n \quad (30)$$

By taking the natural logarithm of Eq. (30)

$$\ln \frac{dx}{dt} = n \ln [C_{A0}(1-x)] + \ln \frac{k}{C_{A0}} = n \ln [C_{A0}(1-x)] + \ln k' \quad (31)$$

where  $k' = \frac{k}{C_{A0}}$ .

#### 4. Thermodynamic analysis

Starting with Eyring-Polanyi equation

$$k = \kappa \frac{k_B T}{h} \exp\left(-\frac{\Delta G}{RT}\right) \quad (32)$$

Taking the natural logarithm of Eq. (32) and setting  $\Delta G = \Delta H - T\Delta S$

$$\ln\left(\frac{k}{T}\right) = -\frac{\Delta H}{R}\left(\frac{1}{T}\right) + \left[\ln \kappa + \ln\left(\frac{k_B}{h}\right) + \frac{\Delta S}{R}\right] \quad (33)$$

where

$\kappa$  is the transmission coefficient and is usually taken as unity.

$k_B = 1.38 * 10^{-23}$  J/K is the Boltzmann constant

$h = 16.63 * 10^{-34}$  J.s is Planck's constant

#### 5. Results and discussions

##### 5.1. The optimization approach

The second order polynomial equation obtained from the response surface methodology (RSM) was fitted with the experimental results. The regression equation with coded parameters is represented as follows:



Table 7

Three independent experiments that validate model adequacy.

Run	Temperature (°C)	Time (min)	Molar ratio	Catalyst (wt%)	Pressure (bar)	Experimental (%)	Predicted (%)
1	240	25	20	0.11	1.20	98.12	99.4
2	240	25	20	0.11	1.20	97.96	99.4
3	240	25	20	0.11	1.20	96.82	99.4

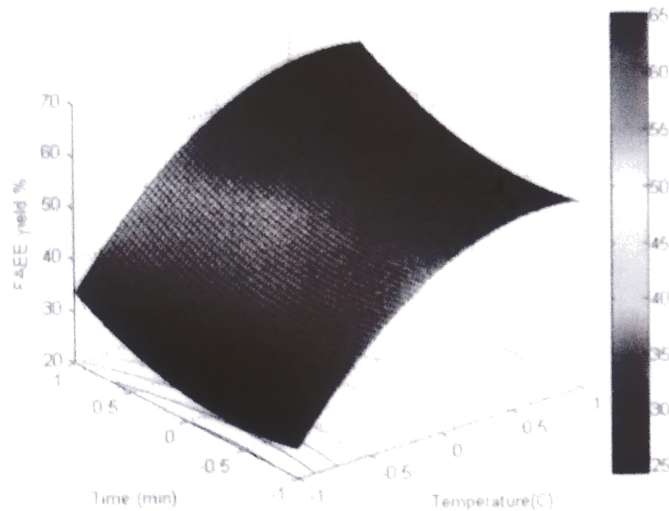


Fig. 9. 3D and contour response surface plot of FAEE yield as a function of temperature and time.

### 5.2. Influence of reaction temperature and reaction time

The reaction temperature represents the most effective parameter among all transesterification reaction parameters. The transesterification reaction was performed under different temperatures (200, 240, and 280 °C) to investigate the effect of the reaction temperature. Fig. 9 illustrates the FAEE yield as a function of the reaction time and temperature. It was observed that increasing the reaction temperature from 200 °C to 240 °C led to a sharp enhancement of FAEE yield (see observation 22 in Table 5) after a short reaction time (25 min). However, further increasing the reaction temperature to 280 °C brought only a slight increase in the FAEE yield because the polyunsaturated fatty acid ester is thermally stable up to 325 °C and starts to decompose around 330 °C. Therefore, the temperature of 280 °C was selected as the maximum reaction point to prevent any chance of the fatty acid ethyl ester thermally degrading and FAEE yield reduction [42].

The influence of the reaction time on the FAEE yield of waste oil under the supercritical process and catalyzed by KOH was investigated by performing the reaction at three different reaction times (see Tables 4 and 5). It is worth saying that the reaction process at 200 °C had achieved the subcritical point, but not supercritical conditions (supercritical ethanol temperature is 240 °C). The analysis of the data shows that the supercritical point is preferable for biodiesel production because there is a sharp increase in the ethyl ester yield after the system achieves the supercritical point [43].

Based on the developed model, all five single parameters, three square parameters, and three quadratic parameters were found to have a significant effect on the yield of FAEE. The significance of each variable can be evaluated according to its p-test value obtained by the analysis of variance (ANOVA). Fig. 9 shows that the FAEE yield in the subcritical region is slightly lower, and the ethyl ester was formed in considerable amounts at supercritical points. Figs. 10 and 11 show the response surface plot of FAEE yield against catalyst wt% and process pressure. As expected, longer reaction times will allow the reaction to proceed towards higher yield.

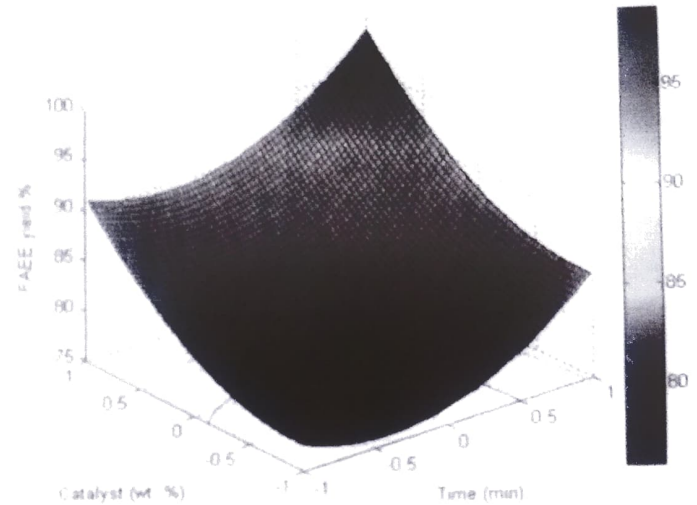


Fig. 10. 3D and contour response surface plot of FAEE yield as a function of time and catalyst.

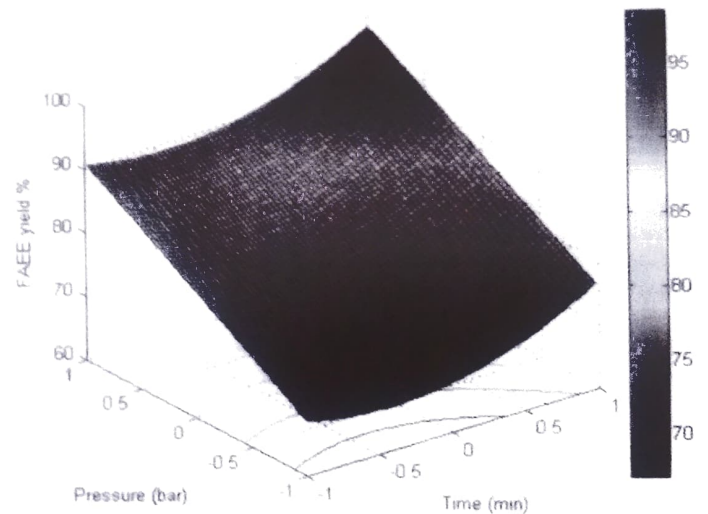


Fig. 11. 3D and contour response surface plot of FAEE yield as a function of time and pressure.

The quadratic coefficients in Eq. (35) indicate the direction that the curve is bending. The negative sign of the quadratic coefficients indicate a convex surface, and the positive quadratic terms indicate a concave surface [44]. Based on the current model (Eq. (35)), the reaction time has the most prominent effect on the biodiesel yield since the reaction time is the only variable that exists in all significant quadratic parameters (i.e.,  $x_1x_2$ ,  $x_2x_4$ , and  $x_2x_5$ ).

### 5.3. Ethanol-to-oil molar ratio

The transesterification reaction stoichiometry is 3 mol of ethanol and 1 mol of oil to produce 3 mol of ethyl ester and 1 mol of glycerol (see Fig. 2). The transesterification reaction is a reversible reaction; therefore, an excess amount of ethanol is needed to shift the forward-

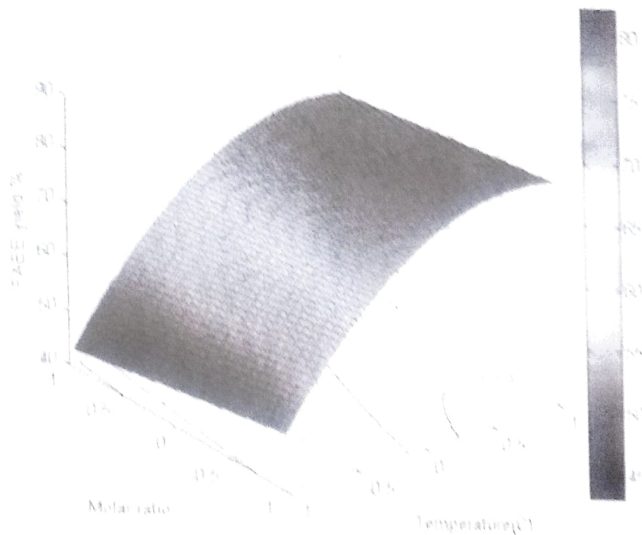


Fig. 12. 3D and contour response surface plot of FAEF yield as a function of temperature and ethanol:oil molar ratio.

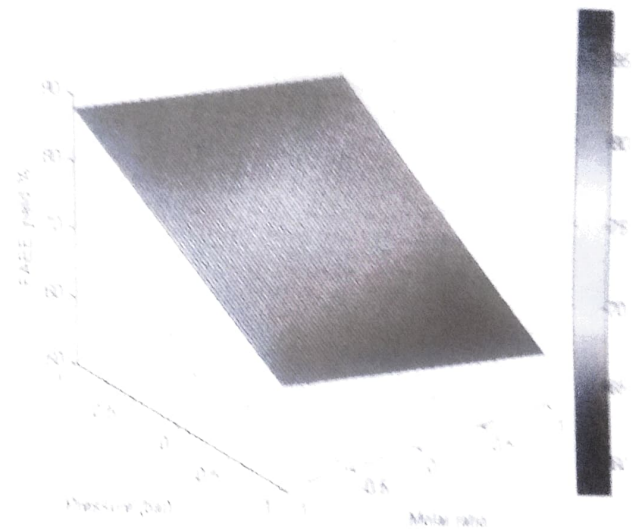


Fig. 14. 3D and contour response surface plot of FAEF yield as a function of ethanol:oil molar ratio and pressure.

reaction and increase the FAEF yield. However, very high ethanol to oil ratio tends to negatively affect the FAEF yield, as shown in Figs. 12, 13, and 14. A reasonable explanation for this phenomenon is that an excess amount of ethanol increases the contact between the ethanol and the oil. However, the solubility of the by-product (i.e., glycerol) in biodiesel also increases, which shifts the reaction equilibrium backwards [45,46].

The molar ratio parameter ( $X_2$ ) represents the less factor that affects the biodiesel yield, since the square and the quadratic coefficients of the molar ratio were not statistically significant, as shown in Eq. (35). Thus, the molar ratio 3D plots look flat, especially in Fig. 14, where the effect of the square and quadratic coefficients vanished.

5.4. Catalyst concentration

The amount of the base catalyst, such as KOH, is vital for the transesterification reaction mainly because of the saponification reaction (see Eq. (12)), which increases the complexity of the product separation step [47]. As shown in Figs. 15 and 16, the FAEF yield increased rapidly as the catalyst amount increased from 0.01 to 0.14 even to the subcritical region (temperature < 240 °C). It can be seen from observation 16 and 23 in Table 5 that the FAEF yield increased

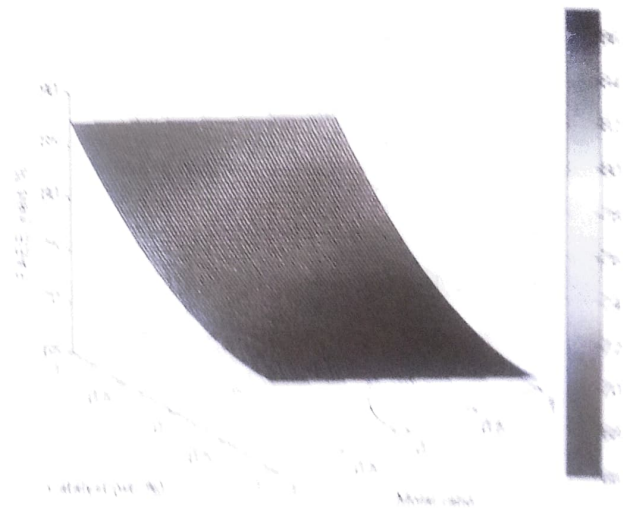


Fig. 18. 3D and contour response surface plot of FAEF yield as a function of ethanol:oil molar ratio and catalyst.

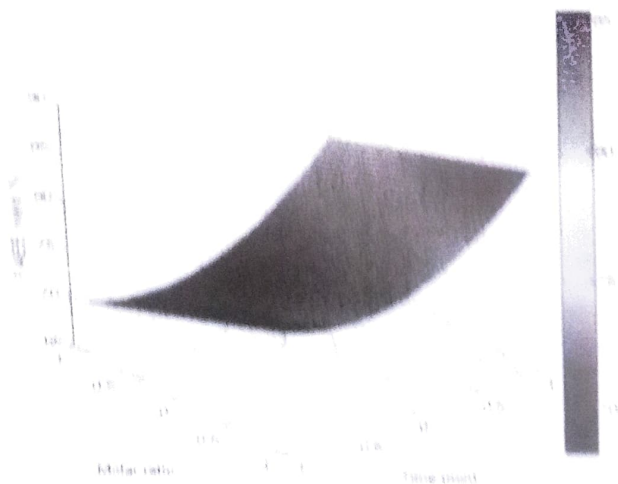


Fig. 14. 3D and contour response surface plot of FAEF yield as a function of time and ethanol:oil molar ratio.

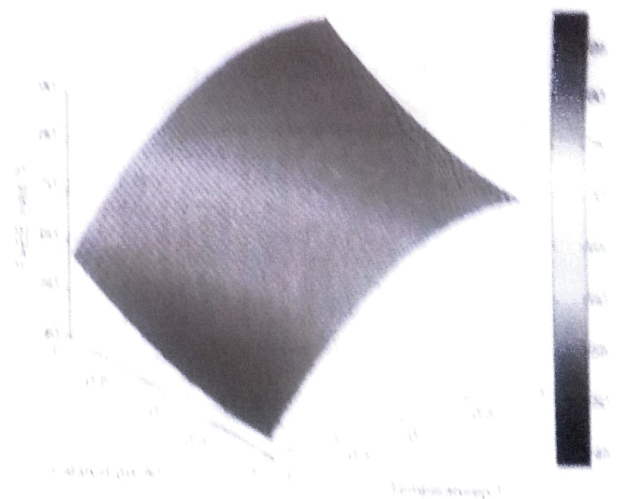


Fig. 16. 3D and contour response surface plot of FAEF yield as a function of temperature and catalyst.

from 71.45% to 80.45% when the KOH amount increased from 0.06 to 0.11. Since these are trace amounts, it may not negatively affect the engine, and due to the dissolution of KOH in the final product, these compounds are not true heterogeneous catalysts. In comparison with the conventional alkali process, the dosage of base catalyst reduced, shortening the reaction time from 150 to 25 min while not increasing the separation cost. This favors cost reduction and enhances process efficiency for large-scale industry practice.

5.5. Reaction pressure

The effect of pressure on the transesterification reaction was optimized at variable temperature, time, ethanol-to-oil molar ratio, and catalyst amount. Based on our previous studies, pressures above 170 bar were not considered due to the low increase in FAEE yield and the high cost for the implementation of such a process. It has been reported that high operation pressure (i.e., higher than 200 bar) may not be industrially viable and increases the cost of biodiesel production. The pressure has a great effect on supercritical fluid properties such as density, viscosity, and the hydrogen bond intensity [28]. When the process pressure was slightly lower than the critical ethanol pressure (64 bar), the FAEE yield increased slightly. However, the yield increased in a more pronounced way at pressures higher than 64 bar, as shown in Figs. 17 and 18. According to observation 22 in Table 5, the best FAEE yield has been obtained at 120 bar. The pressure parameter ( $x_5$ ) does not have significant square coefficients. However, there exists a significant quadratic coefficient of pressure with time, as seen in Eq. (35). The curvature shape of Figs. 17 and 18 occurred due to the significant effect of the square parameters of temperature and catalyst amount.

5.6. Kinetics parameters

The reaction order and reaction rate constants were determined from Eq. (31). It is obvious that the reaction rate constant and reaction order were calculated from the plot of the x-axis equation, which is  $\ln [CA_0(1-x)]$  versus  $\ln dx/dt$  (y-axis). The differential methods of identifying the reaction order using exponential function have been followed. For example, the fitting function of the obtained plot at 200 °C can be expressed as follows:

$$y = 0.8055e^{-(0.04x)} \tag{36}$$

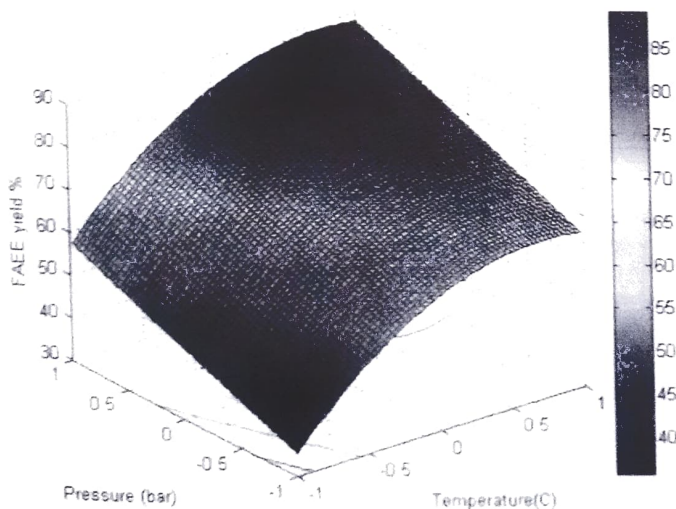


Fig. 17. 3D and contour response surface plot of FAEE yield as a function of temperature and pressure.

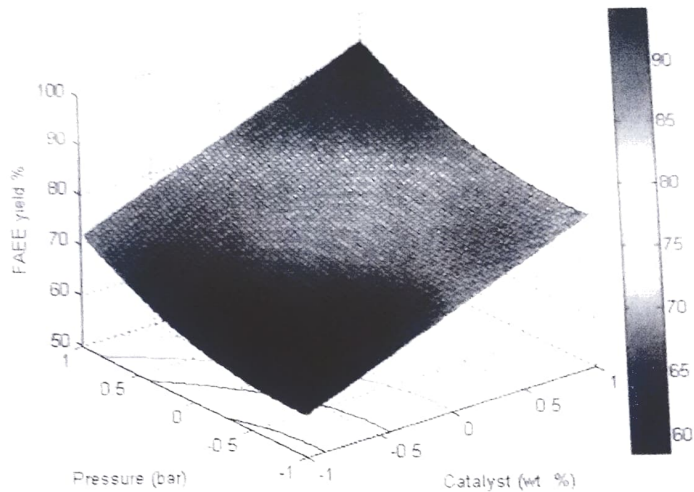


Fig. 18. 3D and contour response surface plot of FAEE yield as a function of catalyst and pressure.

The well-fitted plot of  $\ln dx/dt$  versus  $\ln [CA_0(1-x)]$  was illustrated in Fig. 19, by the straight-line equation:

$$\ln \frac{dx}{dt} = 0.998 \ln [CA_0(1-x)] - 3.523 \tag{37}$$

With an  $R^2$  value of 0.9128, the reaction rate constant is 0.016696. Similarly, the line equation fitting plots of temperatures 240 °C and 280 °C can be calculated with the results listed in Table 8.

5.7. Activation energy and thermodynamic analysis

The Arrhenius equation can be written as follow:

$$\ln k = -\frac{E_a}{RT} + \ln A \tag{38}$$

where  $k$  is the reaction rate constant, and  $E_a$  is the activation energy in kJ/mol.  $R$  is the universal gas constant (8.314 J/mol. K),  $T$  is the absolute temperature in Kelvin, and  $A$  is the pre-exponential factor. The linear correlation between  $\ln k$  and  $1/T$  using the reaction rate constant in Table 8 and the corresponding temperature (i.e., 200 °C, 240 °C, and 280 °C) was illustrated in Fig. 20. The straight line with an  $R^2$  value of 0.9611 was obtained, and the activation energy was calculated from the line slope as  $15.7 \text{ kJ}\cdot\text{mol}^{-1}$ .

The thermodynamic parameters, including Gibbs free energy ( $\Delta G$ ), enthalpy ( $\Delta H$ ), and entropy ( $\Delta S$ ), are important parameters for

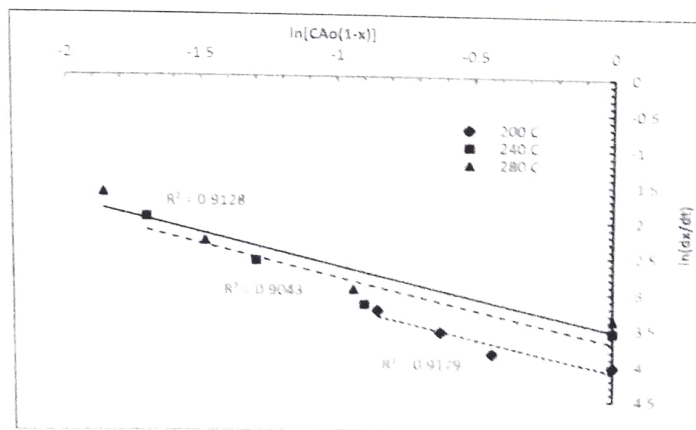


Fig. 19. Plot of  $\ln [CA_0(1-x)]$  vs  $\ln(dx/dt)$ .

**Table 8**  
Reaction rate constant at different temperature.

Temperature (°C)	Rate constant k, min <sup>-1</sup>
200	0.016696
240	0.0251
280	0.029523

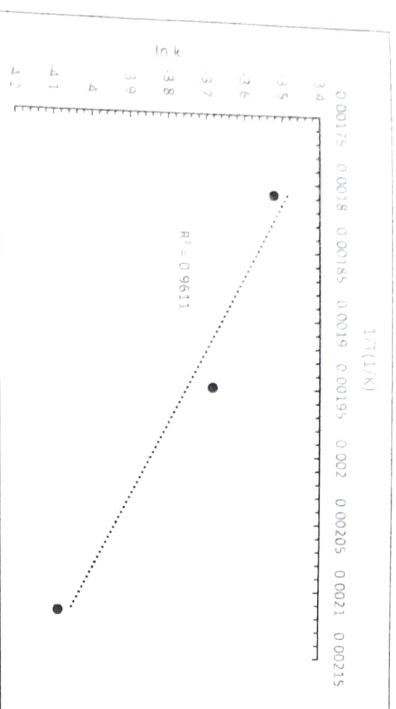


Fig. 20.  $1/T$  plot vs.  $\ln k$ .

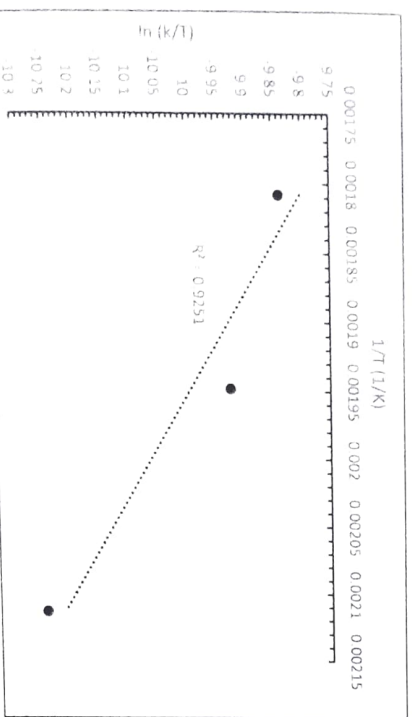


Fig. 21.  $1/T$  plot vs.  $\ln k/T$ .

evaluating the transesterification reaction behavior. The enthalpy and entropy values were calculated by plotting the  $\ln k/T$  vs.  $1/T$  in Eq. (33). As shown in Fig. 21, the  $R^2$  value is 0.9251, and the calculated enthalpy, entropy, and Gibbs free energy are  $11.4 \text{ kJ mol}^{-1}$ ,  $-0.26 \text{ kJ mol}^{-1}$ , and  $144.82 \text{ kJ mol}^{-1}$ , respectively.

## 6. Conclusions

The production of biodiesel from waste cooking oil via supercritical ethanol transesterification using carbon dioxide as a process co-solvent has been conducted in this work. The response surface methodology (RSM) and the analysis of variance (ANOVA) have been successfully applied for designing the parameters of the experiment. The influence of reaction temperature, reaction time, ethanol-to-oil molar ratio, catalyst amount, and pressure on the biodiesel production process has been optimized by (RSM). The optimum process parameters that achieved the 98.12% FAE yield for the supercritical ethanol process are as follows:

- temperature ( $x_1$ ) of 240 °C
- reaction time ( $x_2$ ) of 25 min
- ethanol to oil molar ratio ( $x_3$ ) of 20:1
- catalyst amount ( $x_4$ ) of 0.11 wt%
- pressure( $x_5$ ) of 120 bar

The aim of the current work is to combine the advantages of the super-critical process and alkali catalyzed technologies, such as milder operating conditions, relatively small amounts of catalyst consumption, and enhanced reaction rate. Based on RSM analysis, the order of significance for reaction parameters for biodiesel yield was reaction temperature > catalyst amount > reaction pressure > reaction time > molar ratio. The second-order polynomial regression model was fitted with the experimental results obtained from the experimental design. Finally, the activation energy, Gibbs free energy, enthalpy, and entropy values were calculated as  $15.7 \text{ kJ mol}^{-1}$ ,  $144.82 \text{ kJ mol}^{-1}$ ,  $11.4 \text{ kJ mol}^{-1}$ , and  $-0.26 \text{ kJ mol}^{-1}$ , respectively.

## Symbols and nomenclature

min	minute
kJ	kilojoules
mol	mole
in	inches
ml	milliliters
m	meter
mg	milligrams
$R^2$	process correlation coefficient
adjusted $R^2$	process adjusted coefficient of determination
SCE	super-critical ethanol
FFA	free fatty acid
WCO	waste cooking oil
SS	stainless steel
RSM	response surface methodology
CCD	central composite design
FAEE	fatty acid ethyl ester
ENI 4214	European Committee for Standardization
TG	triglycerides
DG	diglycerides
MG	monoglycerides
G	glycerol
FAE	fatty acid ester
ANOVA	analysis of variance
$F_{2-}$ , $F_{3-}$ , $F_{4-}$ , $F_{1+2-}$ , $F_{1+3-}$ , $F_{1+4-}$	the reactions rate for the forward and reverse reactions in Eqs. (6), (7), and (8) respectively

## CRediT authorship contribution statement

**Aso A. Hassan:** Software, Data curation, Writing - original draft, Visualization, Investigation, Software, Validation. **Joseph D. Smith:** Conceptualization, Methodology, Supervision/author "smith, etien" is not listed as an author of this article and hence cannot be added to the credits section here. please consider moving this content to the acknowledgements section or delete from here..

## Declaration of competing interest

The authors declare that they have no known competing financial interests or personal relationships that could have appeared to influence the work reported in this paper.

## Acknowledgment

We gratefully acknowledge the financial support of the Wayne and Gayle Laidler Foundation for this work.

## References

- [1] Y. Wang, S. Gu, P. Liu, Z. Zhang, Preparation of biodiesel from waste cooking oil via two-step catalyzed process, Energy Convers. Manag. 48 (2007) 184–188.
- [2] M. Keskin, K. Teong, F. Ay, A.R. Mohamed, Homogeneous, heterogeneous and enzymatic catalysis for transesterification of high free fatty acid oil (waste cooking oil)

- to biodiesel: a review. *Bioethanol*. Adv. 28 (2010) 500–518.
- [13] S. Sahana, S. Sadiq, J. Iqbal, I. Ullah, H. Nawaz Bhatti, S. Noorin, H. Ur-Ridman, J. Nisar, M. Iqbal, Biodiesel production from waste cooking oil: an efficient technique to convert waste into biodiesel. *Sustain. Chem. Soc.* 41 (2018) 220–226.
- [14] C. Daniel Mandado de Araújo, C. Cristina de Andrade, E. de Souza e Silva, F. Antonio Dupas, Biodiesel production from used cooking oil: a review. *Renew. Sustain. Energy. Rev.* 27 (2013) 445–452.
- [15] A. Demirtaş, Biodiesel from waste cooking oil via base-catalytic and supercritical methanol transesterification. *Energy Convers. Manag.* 50 (2009) 923–927.
- [16] A. Talebian-Khalkhali, N. Alishah Sadiqia Amin, H. Muzaheri, A review on novel processes of biodiesel production from waste cooking oil. *Appl. Energy* 104 (2013) 663–710.
- [17] J. Dufour, D. Intharoen, Life cycle assessment of biodiesel production from free fatty acid rich waste. *Renew. Energy* 38 (2012) 155–162.
- [18] E. Kerehan, R. Hernandez, W. French, W. Holmes, E. Alley, Biodiesel from activated sludge through in situ transesterification. *J. Chem. Technol. Biochem. Technol.* 85 (2010) 614–620.
- [19] G. Huang, F. Chen, D. Wei, X. Zhang, G. Chen, Biodiesel production by microalgal biotechnology. *Appl. Energy* 87 (2010) 39–46.
- [10] X. Miao, Q. Wu, Biodiesel production from heterotrophic microalgal oil. *Bioresour. Technol.* 97 (2006) 841–846.
- [11] A. Demirtaş, M.F. Demirtaş, Importance of algae oil as a source of biodiesel. *Energy Convers. Manag.* 52 (2011) 163–170.
- [12] A.L. Ahmad, N.H. Mai Yasin, C.J.C. Derek, J.K. Lim, Microalgae as a sustainable energy source for biodiesel production: a review. *Renew. Sustain. Energy. Rev.* 15 (2011) 584–593.
- [13] K. Jalil, R. Guerrero, M.F. Rubens, P.T.V. Rosa, Production of biodiesel from castor oil using sub and supercritical ethanol: effect of sodium hydroxide on the ethyl ester production. *J. Supercrit. Fluids* 83 (2013) 124–132.
- [14] U.S. Department of Energy. [Online]. Available: <http://aide.energy.gov/fuels/>.
- [15] S. Kumar Karim, A. Ghadiri, Preparation of biodiesel from crude oil of *Pongamia pinnata*. *Bioresour. Technol.* 96 (2005) 1425–1429.
- [16] J. Goh, O. Sahu, Development of heterogeneous alkali catalyst from waste chicken eggshell for biodiesel production. *Renew. Energy* 128 (2018) 142–154.
- [17] A. Gulder, P. Singh, F. Ahmad Ansari, B. Singh, F. Bux, Biodiesel synthesis from microalgal lipids using tungstated zirconia as a heterogeneous acid catalyst and its comparison with homogeneous acid and enzyme catalysis. *Fuel* 187 (2017) 180–188.
- [18] M. Di Serio, R. Tesser, M. Dimitroff, F. Cammarota, M. Nestori, F. Santacesaria, Synthesis of biodiesel via homogeneous Lewis acid catalyst. *J. Mol. Catal. A Chem.* 239 (2005) 111–115.
- [19] X. Zhao, F. Qi, C. Yuan, W. Du, D. Liu, Lipase catalyzed process for biodiesel production: enzyme immobilization, process simulation and optimization. *Renew. Sustain. Energy. Rev.* 44 (2015) 182–197.
- [20] Y. He, T. Wu, X. Wang, B. Chen, F. Chen, Cost effective biodiesel production from wet microalgal biomass by a novel two-step enzymatic process. *Bioresour. Technol.* 268 (2018) 583–591.
- [21] J. Yin, Z. Ma, Z. Shang, D. Hu, Z. Xu, Biodiesel production from soybean oil transesterification in subcritical methanol with K3PO4 as a catalyst. *Fuel* 93 (2012) 284–287.
- [22] I.M. Aludash, M.K. Aoua, A. Abdul Aziz, Biodiesel separation and purification: a review. *Renew. Energy* 36 (2011) 437–443.
- [23] J. Liu, Y. Nan, L.L. Taylorides, Continuous production of ethanol based biodiesel under subcritical conditions employing trace amount of homogeneous catalysts. *Fuel* 193 (2017) 187–196.
- [24] E. Martinez Guerra, T. Muppanuri, V. Gunasekar Gude, S. Deng, Non-conventional feedstock and technologies for biodiesel production. *Advanced Solid Catalysts for Renewable Energy Production*, IGI Global, 2018, pp. 96–118.
- [25] G. Srivastava, A. Kumar Paul, V.V. Goud, Optimization of non-catalytic transesterification of microalgae oil to biodiesel under supercritical methanol condition. *Energy Convers. Manag.* 156 (2018) 269–278.
- [26] J. Luc, M.B. Rizkama, F.E. Sertaradjo, Y.H. Ju, S. Ismailji, Production of biodiesel from sea mango (*Cerbera odollam*) seed using in situ subcritical methanol water under a non-catalytic process. *Int. J. Ind. Chem.* 9 (2018) 53–59.
- [27] D.T. Tran, J.S. Chang, D.J. Lee, Recent insights into continuous-flow biodiesel production via catalytic and non-catalytic transesterification processes. *Appl. Energy* 185 (2017) 376–409.
- [28] C.M. Trentin, A.P. Lima, I.P. Alkmin, C. Silva, F. Carillion, M.A. Mazzoni, V.J. Oliveira, Continuous production of soybean biodiesel with compressed ethanol in a microbireactor using carbon dioxide as co-solvent. *Fuel Process. Technol.* 92 (2011) 952–958.
- [29] A. Valverde, L. Demert, F. Recasens, Binary interaction parameters from reacting mixture data. *Supercritical biodiesel process with CO<sub>2</sub> as cosolvent*. *J. Supercrit. Fluids* 143 (2019) 107–119.
- [30] A. Demirtaş, Biodiesel from sunflower oil in supercritical methanol with calcium oxide. *Energy Convers. Manag.* 48 (2007) 937–941.
- [31] L. Wana, H. Liu, D. Skala, Biodiesel production from soybean oil in subcritical methanol using MnCO<sub>3</sub>/ZnO as catalyst. *Appl. Catal. B Environ.* 152–153 (2014) 352–359.
- [32] D.C. Montgomery, *Design and Analysis of Experiments*. John Wiley and Sons, 2001.
- [33] F. Yang, M.A. Hanna, D.B. Marx, R. Sun, Optimization of hydrogen production from supercritical water gasification of crude glycerol byproduct of biodiesel production. *Int. J. Energy Res.* 37 (2013) 1600–1609.
- [34] R.D. Metic, M.D. Tomic, F.E. Kiss, E.B. Nikolic-Djoric, M.D. Simkic, Optimization of hydrolysis in subcritical water as a pretreatment step for biodiesel production by esterification in supercritical methanol. *J. Supercrit. Fluids* 103 (2015) 90–100.
- [35] L.C. Meher, D. Vidya Sagar, S.N. Naik, Technical aspects of biodiesel production by transesterification: a review. *Renew. Sustain. Energy. Rev.* (2006) 248–268.
- [36] F. Maa, M.A. Hannah, Biodiesel production: a review. *Bioresour. Technol.* 70 (1) (October 1999) 1–15.
- [37] Y. Liu, E. Latorra, J.G. Goodwin Jr., Effect of carbon chain length on esterification of carboxylic acids with methanol using acid catalyst. *J. Catal.* 243 (2) (6 September 2006) 221–228.
- [38] G. Vicente, M. Martinez, J. Aracil, A. Esteban, Kinetics of sunflower oil methanolysis. *Ind. Eng. Chem. Res.* 44 (2005) 5447–5454.
- [39] M. Keer, L.M. K. Tee, A.R. Mohamed, Homogeneous, heterogeneous and enzymatic catalysis for transesterification of high free fatty acid oil (waste cooking oil) to biodiesel: a review. *Bioethanol*. Adv. 28 (31 March 2010) 500–518.
- [40] K. Komers, F. Skopal, R. Stokolal, J. Mashek, Kinetics and mechanism of the KOH catalyzed methanolysis of rapeseed oil for biodiesel production. *Eur. J. Lipid Sci. Technol.* 104 (11) (2002) 728–737 November.
- [41] K. Tai Tan, K. Trong Lee, A.R. Mohamed, Optimization of supercritical dimethyl carbonate (SCDMC) technology for the production of biodiesel and value added glycerol carbonate. *Fuel* 89 (2010) 3833–3839.
- [42] T. Muppanuri, H.K. Reddy, P.D. Paul, P. Dairley, C. Adity, S. Deng, Ethanolysis of camellina oil under supercritical condition with hexane as co-solvent. *Appl. Energy* 94 (2012) 84–88.
- [43] B.S. Galdes, C.S. Nunes, P.R. Souza, F.A. Rosa, J.V. Vicentini, O.S. Junior, E.C. Muniz, **Supercritical ethanolysis for biodiesel production from edible oil waste using toluene liquid [HMIml][HSO4] as catalyst**. *Appl. Catal. B Environ.* 181 (2016) 289–297.
- [44] N. Garcia Martinez, P. Andreu Martinez, J. Quezada Medina, A. Perez de los Rios, A. Chica, R. Benito Ruiz, J. Carralada Abril, Optimization of non-catalytic transesterification of tobacco (Nicotiana glauca) seed oil using supercritical methanol to biodiesel production. *Energy Convers. Manag.* 131 (2017) 99–108.
- [45] D. Zeng, L. Yang, T. Fang, Process optimization, kinetic and thermodynamic studies on biodiesel production by supercritical methanol transesterification with CH<sub>3</sub>CO<sub>2</sub>N catalyst. *Fuel* 203 (2017) 739–748.
- [46] F. Gunawan, A. Kurniawan, I. Gunawan, Y. H. Ju, A. Ayucitra, F.E. Sertaradjo, S. Ismailji, Synthesis of biodiesel from vegetable oils wastewater sludge by in situ subcritical methanol transesterification: process evaluation and optimization. *Biomass Bioenergy* 69 (2014) 28–38.
- [47] J.Z. Yin, M. Xiao, A.Q. Wang, Z.L. Xu, Synthesis of biodiesel from soybean oil by coupling catalysis with subcritical methanol. *Energy Convers. Manag.* 49 (2008) 3512–3516.